Cell-Free Urine and Plasma DNA Mutational Analysis Predicts Neoadjuvant Chemotherapy Response and Outcome in Patients with Muscle-Invasive Bladder Cancer

Emil Christensen[1,2], Iver Nordentoft[1], Karin Birkenkamp-Demtröder[1,2], Sara K. Elbæk[2], Sia V. Lindskrog[1,2], Ann Taber[1,2], Tine G. Andreasen[1,2], Trine Strandgaard[1,2], Michael Knudsen[1], Philippe Lamy[1], Mads Agerbæk[3], Jørgen B. Jensen[2,4], and Lars Dyrskjøt[1,2]

ABSTRACT

Purpose: To investigate the use of plasma and urine DNA mutation analysis for predicting neoadjuvant chemotherapy (NAC) response and oncological outcome in patients with muscle-invasive bladder cancer.

Experimental Design: Whole-exome sequencing of tumor and germline DNA was performed for 92 patients treated with NAC followed by radical cystectomy (RC). A custom NGS-panel capturing approximately 50 mutations per patient was designed and used to track mutated tumor DNA in plasma and urine. A total of 447 plasma samples, 281 urine supernatants, and 123 urine pellets collected before, during, and after treatment were analyzed. Patients were enrolled from 2013 to 2019, with a median follow-up time of 41.3 months after RC.

Results: We identified tumor DNA before NAC in 89% of urine supernatants, 85% of urine pellets, and 43% of plasma samples. Tumor DNA levels were higher in urine supernatants and urine pellets compared with plasma samples ($P < 0.001$). In plasma, detection of circulating tumor DNA (ctDNA) before NAC was associated with a lower NAC response rate ($P < 0.001$). Detection of tumor DNA after NAC was associated with lower response rates in plasma, urine supernatant, and urine pellet ($P < 0.001$, $P = 0.03$, $P = 0.002$). Tumor DNA dynamics during NAC was predictive of NAC response and outcome in urine supernatant and plasma ($P = 0.006$ and $P = 0.002$). A combined measure from plasma and urine supernatant tumor DNA dynamics stratified patients by outcome ($P = 0.003$).

Conclusions: Analysis of tumor DNA in plasma and urine samples both separately and combined has a potential to predict treatment response and outcome.

Introduction

Localized muscle-invasive bladder cancer (MIBC) is a common malignancy with approximately 570,000 cases diagnosed globally in 2020 (1). The standard treatment regimen is neoadjuvant chemotherapy (NAC) followed by radical cystectomy (RC); however, approximately 50% of patients experience disease recurrence following surgery (2). The current NAC response evaluation consists of a pathological assessment of the surgically removed bladder and adjacent lymph nodes, and thereby inherently lacks the potential to identify patients where a change in treatment regimen might be favorable. Recent studies have identified improved outcomes for patients responding to NAC, in particular if pathological complete response (pCR, pT0N0) is achieved (3). However, meta-analyses have observed pCR in only approximately 25% of patients and pathological downstaging (= <pTisT0TaN0) in approximately 50% and considerable overtreatment might therefore be taking place (4, 5). In addition, a large meta-analysis identified a 5% improved survival rate for patients treated with NAC compared with non-treated patients (6). Studies using a tumor-centric approach for prediction of NAC response have identified genomic alterations in DNA damage repair pathways and genomic instability to be associated with an increased likelihood of response (7–10). Gene expression subtypes have also been associated with NAC response; however, conflicting results have been reported (10–13). No molecular markers have yet entered into clinical practice, although a clinical trial aiming to demonstrate an association between NAC response and mutations in DNA damage repair pathways is ongoing (NCT03609216).

Circulating tumor DNA (ctDNA) has emerged as a powerful biomarker reflecting tumor invasiveness and patient outcome in multiple cancers, including MIBC (14–17). We recently demonstrated that ctDNA dynamics in plasma samples during treatment with NAC reflect treatment response, indicating that ctDNA measurements during treatment could provide a measure of response before RC is carried out (18). A study by Chauhan and colleagues (19) investigated urinary tumor–derived DNA (utDNA) from samples collected before RC and identified higher levels among patients without NAC response compared with those with response. Patel and colleagues (20) have similarly demonstrated persistence of utDNA during NAC to be associated with recurrence after RC. However, previous studies focusing on NAC response and urine samples have been conducted in small cohorts. Here, we present a larger study on 92 patients with MIBC

[1]Department of Molecular Medicine, Aarhus University Hospital, Aarhus, Denmark. [2]Department of Clinical Medicine, Aarhus University, Aarhus, Denmark. [3]Department of Oncology, Aarhus University Hospital, Aarhus, Denmark. [4]Department of Urology, Aarhus University Hospital, Aarhus, Denmark.

E. Christensen and I. Nordentoft contributed equally as co-first authors of this article.

Corresponding Author: Lars Dyrskjøt, Aarhus University Hospital, Palle Juul-Jensens Boulevard 99, Aarhus N, 8200 Denmark. Phone: 45-7845-5320; E-mail: lars@clin.au.dk

Clin Cancer Res 2023;29:1582–91

doi: 10.1158/1078-0432.CCR-22-3250

This open access article is distributed under the Creative Commons Attribution-NonCommercial-NoDerivatives 4.0 International (CC BY-NC-ND 4.0) license.

©2023 The Authors; Published by the American Association for Cancer Research

Translational Relevance

About 45% of patients with localized muscle-invasive bladder cancer treated with neoadjuvant chemotherapy (NAC) and radical cystectomy will develop metastasis within 2 years. The predictive value of monitoring cell-free urine DNA in this setting has not been investigated, and the added value of combined plasma DNA analysis is currently not known. Here, we report a combined tumor-informed analysis of urinary and plasma DNA mutations to investigate the potential for NAC response and outcome prediction.

focusing on analysis of tumor DNA in paired plasma and urine samples to investigate the potential for NAC response prediction.

Materials and Methods

Patient cohort

A total of 92 patients treated with NAC before RC were prospectively enrolled between 2014 and 2019 at Aarhus University Hospital (Aarhus, Denmark). Treatment and surveillance was done in accordance with Danish national guidelines, as previously described (18). Whole-exome sequencing (WES) and plasma data for 56/92 patients were generated previously (18). Summarized metrics for WES data is available in Supplementary Table S1. Pathological downstaging, as evaluated from the RC specimen, was defined as pT0/Ta/TisN0. Only patients with plasma and/or urine supernatants and/or urine pellets were included in the study. Detailed follow-up data were available for all patients (Supplementary Table S2). Recurrence data were obtained from CT scans or pathology reports and survival data were obtained from the nationwide civil registry. All patients provided informed written consent, and the study was approved by The National Committee on Health Research Ethics (#1302183). Study data were collected and managed using REDCap hosted at Aarhus University (21, 22).

Clinical samples

Tissue samples for WES were obtained from transurethral resection of the bladder (TURB) at the time of diagnosis ($n = 90$) or from RC specimens ($n = 2$). In addition, 32 tissue samples from RC specimens, with paired TURB tissue available, were included for mutation tracking over time. DNA was extracted from sections of Tissue-Tek O.C.T Compound-embedded tissue or punches of formalin-fixed paraffin-embedded tissue (FFPE) using a Puregene DNA purification kit (Gentra Systems), the QIAamp DNA FFPE tissue kit or Allprep DNA/RNA Kit (QIAGEN). Leukocyte DNA was extracted from the buffy coat from all patients using the QIAsymphony DSP DNA midi kit (QIAGEN). Urine and plasma sample processing, storage, and DNA extraction were performed as previously described (18, 23, 24). A median of 4 mL plasma (range, 2.5–4 mL) and 4 mL urine supernatant (range, 2.9–5 mL) was used for extraction of cell-free DNA (cfDNA) yielding a median of 9.0 ng/mL for plasma samples and 1.7 ng/mL for urine supernatants.

WES

WES was performed using Twist Enzymatic Fragmentation Library prep and Human Core Exome Capture kit. Samples were sequenced on an Illumina Novaseq 6000. Samples from 56 patients included from Christensen and colleagues (18), were subjected to library preparation using Kapa HyperPrep and captured using SeqCap EZ MedExome or MedExomePlus. These samples were sequenced on an Illumina NextSeq 500. Raw sequencing data were initially processed using bcl2fastq2 and Trim Galore!/cutadapt (hg19/hg38 processing, CRAN, RRID: SCR_011847). FastQ files were processed according to the GATK Best Practices (25): Alignment using bwa-mem, marking of duplicate reads using Picard, base recalibration using GATK(RRID: SCR_001876), quality metrics were assessed using Picard. Mutations were identified using MuTect2 with default parameters except the threshold for maximum alternate alleles in the germline was raised. A custom filter selecting variants only vastly more present in the tumor and in regions with low noise, was subsequently applied (26). Furthermore, variants identified by MuTect2 that did not pass the built-in filters were reintroduced if they were identified with high confidence using VarScan2/Strelka (hg19/hg38 processing, https://github.com/Jeltje/varscan2; refs. 27, 28). All somatic alterations were annotated using annovar (29). Summarized metrics for WES data is available in Supplementary Table S1.

Liquid biopsy sequencing and tumor DNA detection

To increase sequencing depth, and simultaneously limit sequencing costs, the patient cohort was split in two before patient-specific panel design. Two panels were designed on the basis of WES data for each subcohort. Panel 1 covered a total of 2,474 unique genomic positions (50 patients), resulting in 50 positions of interest per patient. Panel 2 covered a total of 2,087 unique genomic positions (42 patients), resulting in 43–50 positions of interest per patient. Using 2 panels instead of one increased the sequencing depth and reduced the sequencing cost by approximately 50%. DNA extracted from liquid biopsies was subjected to Twist Bioscience Mechanical Fragmentation Library preparation. The adapters were replaced with xGen UDI-UMI adapters (Integrated DNA Technologies) to incorporate unique molecular identifiers (UMI) for reducing the error rate. DNA extracted from urine pellets was fragmented before library preparation to a fragment size of approximately 350 bp using the Twist Library Preparation Enzymatic Fragmentation Kit 1.0 (Twist Bioscience). A median DNA input of 39.5 ng (range, 5.7–258 ng), 50 ng (range, 4–50 ng), and 7.6 ng (range, 0.2–110 ng) was used for library preparation for plasma samples, urine pellets, and urine supernatants, respectively. The enrichment process was carried out using Twist Bioscience Target Enrichment Protocol and the described custom panels. The libraries were paired end sequenced (2×150 bp) on the illumina NovaSeq 6000 sequencer. UMI consensus base calls were performed using the fgbio tool package(http://fulcrumgenomics.github.io/fgbio/; ref. 30). Samples were sequenced to median target coverages of 3,346X, 1,560X, and 2,588X for plasma, urine pellet, and urine supernatant, respectively, after UMI consensus collapsing. The overlapping parts of read pairs were only counted once.

Custom panel design

For selection, mutations were initially filtered to enrich statistically convincing mutations. A maximum of 1 mutation-containing read was allowed in the associated germline unless at least 20 times as many mutation-containing reads were identified in the tumor sample. Furthermore, a minimum read-depth of 10 for both the tumor and germline samples was set. We leveraged previously generated sequencing data using identical sequencing chemistry, but different genomic positions targeted (described in ref. 31). C>T/G>A mutations were frequently observed at positions with no expected mutations. In addition, the trinucleotide contexts "NCG" and "CGN" were frequently mutated. In samples from patients with MIBC, C>T mutations are

the most commonly observed accounting for 51% of mutations in TCGA data (32). Therefore, the top 10 mutations per patient based on the log odds score derived from Mutect2 (33), reflecting the probability of the variant being a true mutation, were prioritized regardless of the mutational context. Furthermore, up to 10 mutations assessed as damaging (Polyphen2: possibly/probably damaging or MutationAssessor: medium/high; refs. 34, 35), were included per patient in the panel. These were prioritized on the basis of the variant allele frequency (VAF) and only included if the VAF was above the 1st quartile for the VAF of the sample in question to limit the selection of subclonal mutations. Similarly, up to 10 mutations in genes associated with bladder cancer [bladder cancer driver genes from (ref. 36) and significantly mutated genes in (ref. 32)] were selected if the VAF was above the 1st quartile. In addition, two TERT promoter mutations, which are frequently observed in patients with bladder cancer (37), were added to both panels. Collectively, the mutation selection process thereby serves to limit the error-rate of included genomic positions while optimizing the mutation selection to contain the mutations most likely to be clonal and impactful. Panel 1 was designed on the basis of hg19-aligned WES data and panel 2 was designed on the basis of hg38-aligned WES data. For comparative analyses, the panel 1 positions were carried over to hg38 using the R package rtracklayer (38).

Custom panel variant calling pipeline

The inclusion of genomic positions associated with multiple patients on every custom panel facilitates an abundance of sequencing data for every genomic position with no mutations expected to be present. These data can serve to build a background error model. To achieve this, we used an analysis framework based on a maximum likelihood implementation of the shearwater algorithm developed by Gerstung and colleagues (39). Data generated from liquid biopsy samples were initially split by sample type before generating error models. For analysis of mutations for every patient, all data generated for a liquid biopsy type were loaded and other samples originating from the same patient were discarded. Following, the genomic positions associated with a patient were selected and base counts were generated for all samples of the given type. Only reads with a minimum mapping quality of 20 and bases with a minimum quality of 20 were considered. The presumably non-mutated data were fitted to a binomial distribution with site-specific calculation of the dispersion, as described by Gerstung and colleagues (39). Presumably mutated data, that is, data from the target patient, were assessed for a statistical significant difference compared with the background error model, resulting in *P* values. Only base changes expected on the basis of the mutation selection for the target enrichment were considered. Samples with a VAF above 25% were excluded when generating the error-model. Genomic positions with an average VAF above 10% across all considered samples and/or a read-depth below 50 in the target sample were excluded. *P* values were corrected for multiple testing using the Benjamini–Hochberg procedure and adjusted *P* values below 0.05 were considered significant.

The sample-wise tumor-derived DNA (tdDNA) signal strength was assessed using the Fisher's method on the target positions of a given patient and compared with the results of the Fisher's method applied to a random selection of 50 mutations of all non-target mutations in the panel 10,000 times. A sample was categorized as tdDNA positive only if the results of the Fisher's method were the relatively strongest when compared with the 10,000 random selections. Mean sample VAF was defined as the mean VAF of all mutations that were significant after adjusting for multiple testing. For samples with no significant mutations after adjusting for multiple testing, but with a sample-wise positive tdDNA call, the mean sample VAF was defined as the mean VAF for all mutations with unadjusted *P* values below 0.1.

Estimation of limit of detection

We generated *in silico* sample counts to assess the limit of detection (LOD) at every position for all included sample types. To accomplish this, we performed the initial steps of the shearwater-based calling algorithm (39), but replaced the counts from the target sample with *in silico* counts representing 1–25 reads. A random sample was used to

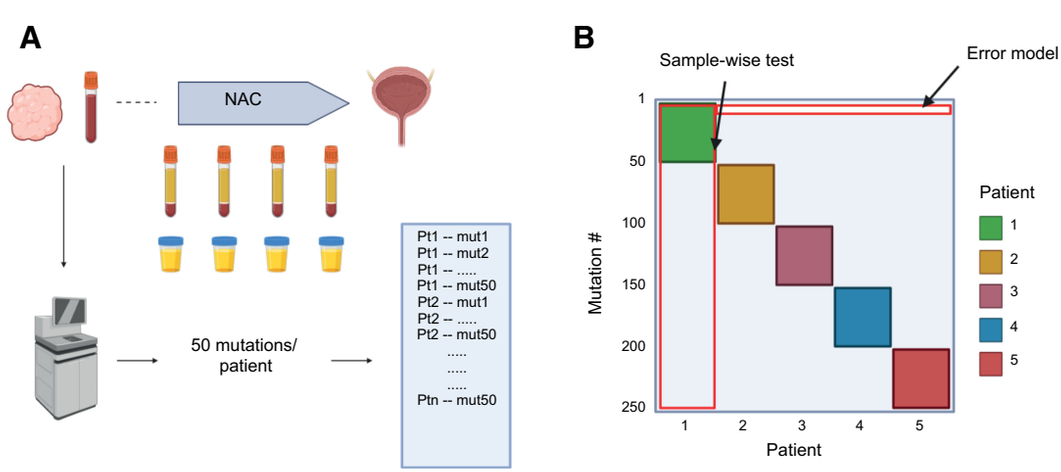

Figure 1.

Study and methodology overview. **A,** The study includes patients treated for muscle-invasive bladder cancer (MIBC). Upon diagnosis, a tumor sample obtained from transurethral resection of the bladder and a germline sample were subjected to whole-exome sequencing (WES). Approximately 50 somatic variants were selected per patient for design of two custom NGS panels based on 50 and 42 patients. Plasma and urine samples were collected before, during, and after treatment with neoadjuvant chemotherapy. **B,** Illustration of the custom panel NGS data, exemplified using only five patients. For every single mutation, an error model was constructed on the basis of data from the samples not associated with that given mutation. This was used to test for significance in the sample associated with that given mutation. Furthermore, a sample-wise test was performed for every sample by applying the Fisher's method to *P* values obtained for all mutations associated with that sample. A random selection of 50 other mutations from the panel not associated with the given sample was similarly assessed using the Fisher method. This was repeated 10,000 times, and only samples with a score higher than all random selections were considered tumor DNA positive. (Created with BioRender.com.)

determine ratios between forward and reverse read depth for every position. The remainder of the calling pipeline was then carried out and the minimum number of reads required to reach statistical significance was determined for every position. On the basis of the predetermined read depth of the *in silico* sample, the LOD was then calculated (Supplementary Fig. S1). The specified LODs for the different sample types were inferred on the basis of the mean LOD for the closest of the queried read depths. In addition, the LOD varied across the different base changes with C>T demonstrating the poorest LOD (Supplementary Fig. S1, read depth fixed at 3,000X).

Assessment of changes in the tumor mutational landscape during NAC

We performed WES of DNA from tumor tissue obtained from RC specimens for 32 patients to assess the mutational changes that occurred during treatment with NAC. We observed a median of 708 mutations in these tumors and a median of 1,295 mutations in the associated primary tumors. Only an average of 16.4% of mutations observed in primary tumors were detected in tumors from RC specimens, underlining the importance of selecting mutations from treatment naive tumors (Supplementary Fig. S2). Similarly, a median of 19 (IQR, 0–31) of the panel mutations were identified in RC tumors, probably caused by a lower tumor cell percentage in RC tumors as reflected by lower 90th percentile VAFs (Supplementary Fig. S2).

Statistical analyses

Statistical significance was assessed by performing a Wilcoxon rank-sum test for continuous non-paired variables, a Wilcoxon signed rank-sum test for continuous paired variables and a Fisher's exact test for

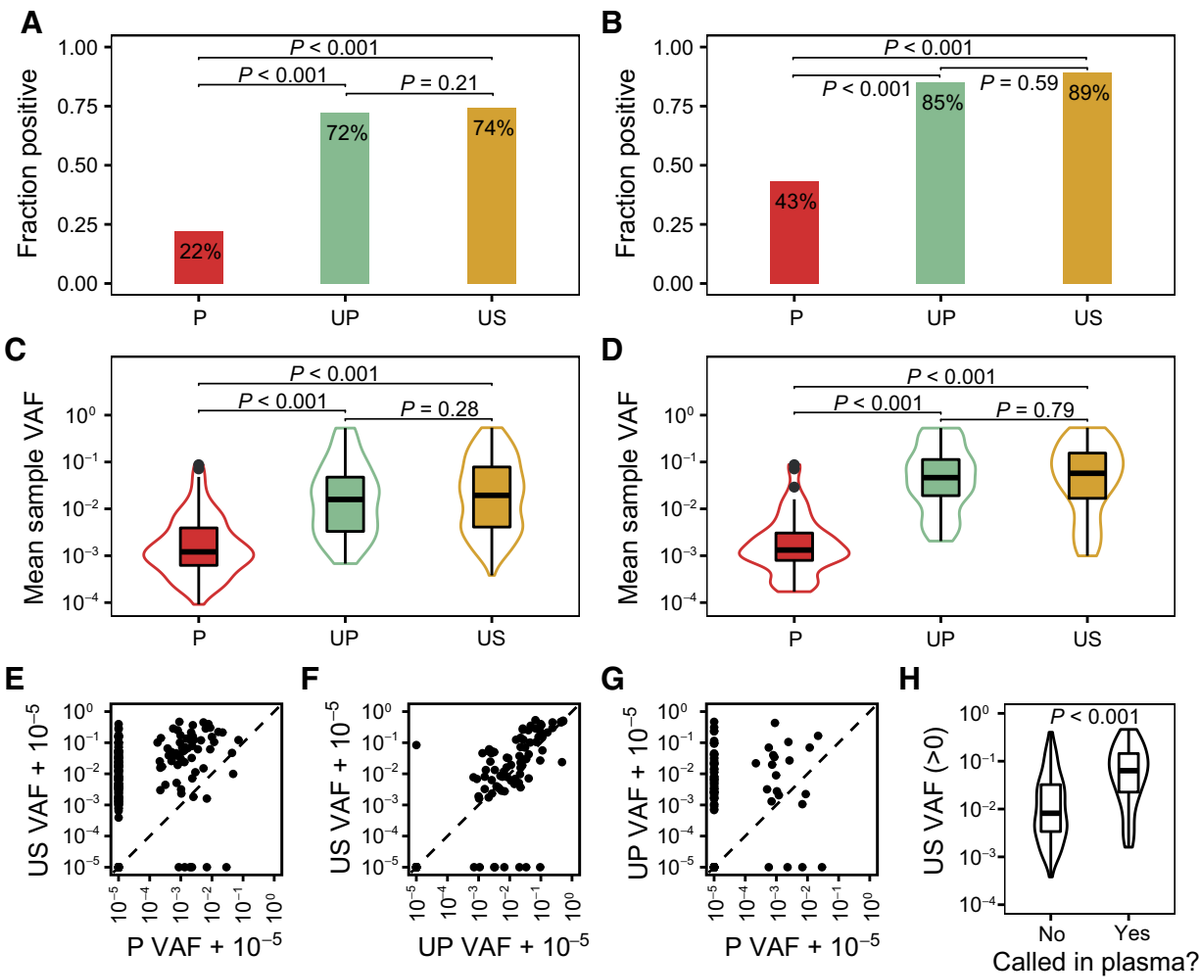

Figure 2.

Measurements of tumor DNA across sample types. **A** and **B,** The fraction of samples positive for tumor DNA by sample type. **A,** All samples (P, $n = 99/447$; UP, $n = 89/123$; US, $n = 209/281$) and (**B**) samples collected before neoadjuvant chemotherapy (NAC; P, $n = 52/120$; UP, $n = 40/47$; US, $n = 82/92$). **C** and **D,** Mean sample VAF levels for samples with detectable tumor DNA split by sample type. **C,** All samples (P, $n = 99$; UP, $n = 89$; US, $n = 209$) and (**D**) samples collected before NAC (P, $n = 52$; UP, $n = 40$; US, $n = 82$). *P* values were calculated using a Wilcoxon rank-sum test. **E–G,** Mean sample VAF levels for comparison of all sample types. Only samples from clinical visits with at least 2 sample types available were included. **H,** Mean sample VAF level for urine supernatants split by ctDNA call status (348 not called and 99 called) in plasma samples from the same clinical visit. Only samples with detectable utDNA in urine supernatants were considered. *P* values were calculated using a Wilcoxon rank-sum test. P, plasma; UP, urine pellet; US, urine supernatant.

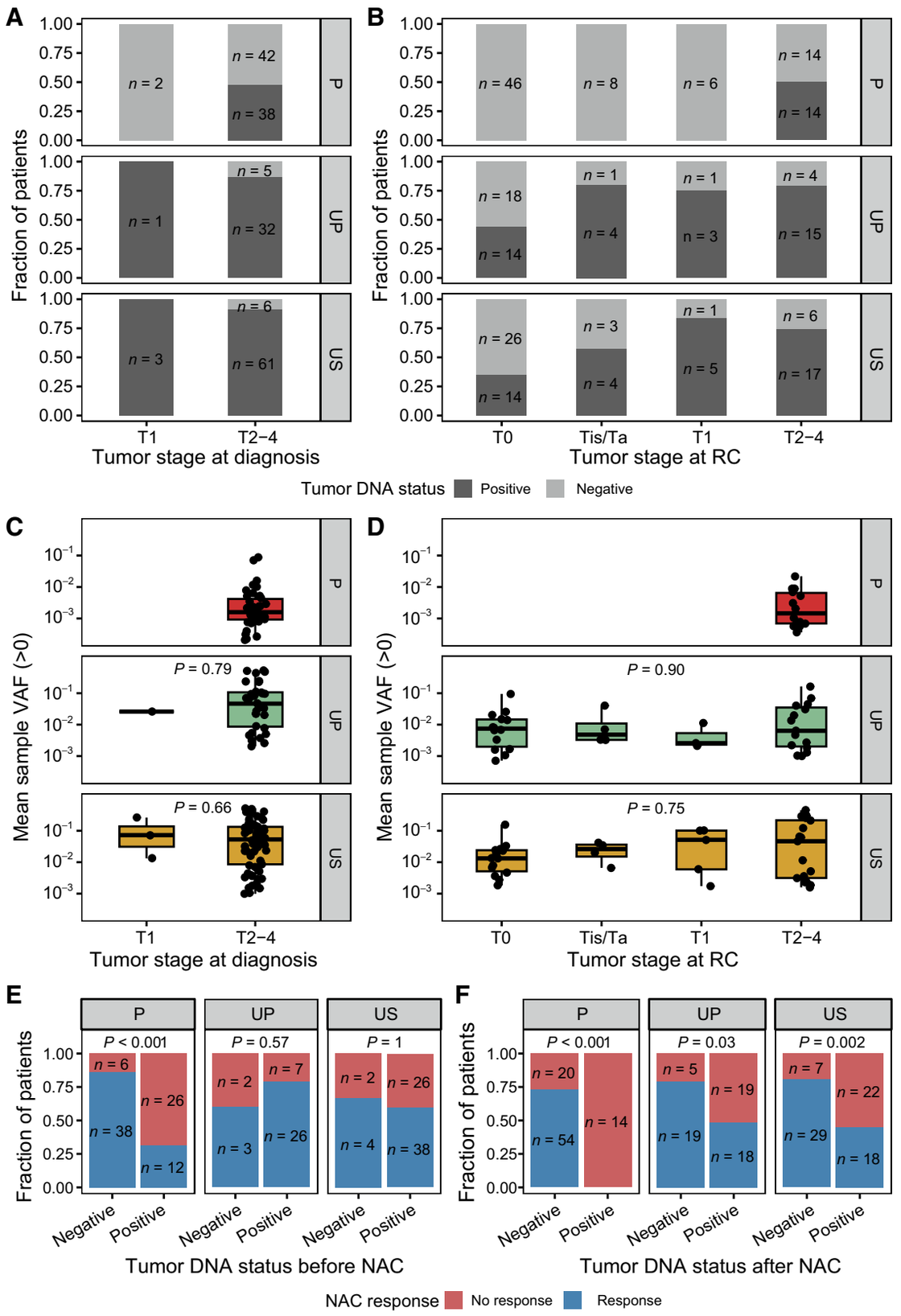
A
B
C
D
E
F
Fraction of patients
Mean sample VAF (>0)
P
UP
US
T1
T2–4
Tumor stage at diagnosis
T0
Tis/Ta
Tumor stage at RC
Tumor DNA status
Positive
Negative
P = 0.79
P = 0.66
P = 0.90
P = 0.75
P < 0.001
P = 0.57
P = 1
P < 0.001
P = 0.03
P = 0.002
Tumor DNA status before NAC
Tumor DNA status after NAC
NAC response
No response
Response

categorical variables. Sample level assessment of tumor DNA status was performed using the Fisher's method. Survival analyses were carried out in R using packages survminer and survival (https://cran.r-project.org).

Data availability

The raw sequencing data generated in this study are not publicly available as this compromises patient consent and ethics regulations in Denmark. Processed non-sensitive data are available upon reasonable request from the corresponding author.

Results

Patients and methodology

In total, 92 patients treated with NAC for MIBC were included in the study. Ninety-one patients underwent RC after NAC and 61% showed pathological downstaging (53% complete response, pT0N0). Median follow-up after RC was 41.3 months. Tumor and germline DNA was subjected to WES for identification of somatic variants with a median target coverage of 114X for tumor and 73X for germline samples. The study builds on previously published tissue-based WES and plasma sample-based data for 56 patients (18). Here, we extended the cohort with an additional 36 patients with plasma-based analyses ($n = 159$) and included urine supernatant ($n = 281$) and urine pellet ($n = 123$) analyses (Supplementary Fig. S1). For the extended cohort and new samples, we used a tumor-informed patient-specific strategy for detection of tumor DNA based on selection of approximately 50 mutations per patient from WES data for design of a custom NGS panel (**Fig. 1A**). Consequently, all selected mutations were patient-specific and were not shared between patients. Plasma and urine-based samples were subsequently subjected to targeted sequencing. Analysis of tumor DNA was performed on a mutation-wise level based on error-models of all relevant genomic positions and an integrated sample-level assessment for tumor DNA positivity (**Fig. 1B**). The LOD was determined to be approximately 0.05%, 0.10%, and 0.09% for plasma, urine pellet, and urine supernatant, respectively (Supplementary Fig. S1).

Tumor DNA detection across sample types

The tumor DNA detection frequency varied between sample types and was higher in urine supernatants and pellets compared with plasma samples (**Fig. 2A**). For tumor DNA-tracking purposes (tumor DNA dynamics), detection of tumor DNA before initiation of NAC is necessary, and here we similarly observed tumor DNA to be present more frequently in urine supernatants and pellets compared with plasma samples (**Fig. 2B**). In line with this observation, we found the level of tumor DNA to be higher in urine supernatants and pellets compared with plasma samples both when considering all samples and only samples before NAC (**Fig. 2C** and **D**).

Urine supernatants and plasma demonstrated a weak correlation and a sample concordance in tumor DNA status of 46.0%, with urine supernatants more often containing utDNA compared with plasma (rho = 0.41, **Fig. 2E**). Tumor DNA levels in urine supernatants and urine pellets were highly correlated and 91.7% of samples were concordant in terms of tumor DNA status (rho = 0.78, **Fig. 2F**).

Urine pellet tumor DNA status also showed a weak correlation to plasma, as expected (43.1% concordance, rho = 0.15, **Fig. 2G**). Interestingly, for visits with ctDNA presence in plasma, the associated urine supernatants displayed significantly higher levels of utDNA (**Fig. 2H**), which could be an indication of renal clearance of ctDNA from the plasma or simply a reflection of a large invasive tumor. However, no other comparisons with adjustment for tumor DNA status were significant (Supplementary Fig. S3).

We investigated whether the tumor DNA assay performance was highly dependent on the amount of extracted DNA and, more importantly, on the library input. Importantly, we did not find that tumor DNA positivity was associated with higher amounts of DNA input (Supplementary Figs. S4 and S5).

We analyzed urine dipstick data that were collected at the same time as urine supernatants to investigate urine parameters affecting DNA mutation calling. On the basis of 72 cases of paired urine supernatant and urine dipstick data, we identified the levels of leukocytes, nitrite, protein, and erythrocytes to be associated with the level of cfDNA (Supplementary Fig. S6). However, only the level of erythrocytes was associated with the tumor DNA positive call status of samples and the level of tumor DNA (Supplementary Figs. S7 and S8), indicating that DNA mutation calling was not affected with wild-type DNA contamination. Furthermore, it indicated that patients with blood in the urine may have a higher tumor burden.

Tumor DNA measurements compared with tumor burden and patient outcome

We observed ctDNA plasma sample positivity in 46% and 50% of visits with concurrent T2–4 tumors before and after NAC, respectively (**Fig. 3A** and **B**). Of note, only samples drawn from patients with muscle-invasive tumors at diagnosis and at the time of RC were positive for plasma ctDNA (**Fig. 3A** and **B**). In urine pellets and urine supernatants, tumor DNA sample-positivity rates before NAC were 86% and 91% for T2–4 tumors, respectively (**Fig. 3A**), and varied across tumor stages after NAC (**Fig. 3B**).

Sensitivity and specificity measures for urine pellet and urine supernatant analyses for detection of residual tumor were relatively low, and probably highlights that urine may be more or less concentrated, with variable test results as a consequence (UP: sensitivity = 79%; specificity = 56%: US: sensitivity = 72%; specificity = 65%).

In urine-based samples, the levels of tumor DNA were equal across tumor stages (**Fig. 3C** and **D**). This could be due to urine-based tumor DNA primarily reflecting tumor exposure in the bladder lumen and less so the invasiveness of the tumor. In line with this, tumor DNA was always detected in both urine supernatants and pellets, when only

Figure 3.
Tumor DNA status before and after neoadjuvant chemotherapy compared with tumor stage and outcome. **A** and **B,** Fraction of patients positive for tumor DNA split by sample type and tumor stage. **A,** Tumor stage evaluation based on transurethral resection of the bladder (TURB) specimen and tumor DNA status based on samples collected before NAC. **B,** Tumor stage evaluation based on radical cystectomy (RC) specimen and tumor DNA status based on samples collected after NAC and before RC. **C** and **D,** Mean sample VAF levels for all patients with detectable tumor DNA split by sample type and tumor stage. **C,** Tumor stage evaluation based on TURB specimen and tumor DNA level based on samples collected before NAC. *P* values were calculated using a Wilcoxon rank-sum test. **D,** Tumor stage evaluation based on RC specimen and tumor DNA level based on samples collected after NAC and before RC. *P* values were calculated using a Kruskal–Wallis test. **E** and **F,** Tumor DNA status compared with response to treatment with NAC for all analyzed sample types. **E,** Tumor DNA status determined before NAC. **F,** Tumor DNA status determined after NAC.

considering samples collected before TURB (Supplementary Fig. S9). In addition, we observed an association between NAC response and plasma ctDNA status both before and after NAC, and only after NAC for urine supernatants and urine pellets (**Fig. 3E** and **F**). Only plasma ctDNA status before and after NAC was associated with recurrence-free survival (RFS; Supplementary Fig. S10). Dichotomization of samples based on sample-type–specific median VAFs, demonstrated an association between the level of ctDNA and NAC response for plasma collected both before and after NAC, but not for tumor DNA from urine supernatants and pellets (Supplementary Fig. S11). The level of ctDNA in plasma samples collected both before and after NAC and for utDNA in urine supernatants after NAC was furthermore associated with RFS (Supplementary Fig. S12).

Tumor DNA liquid biopsy dynamics and treatment response

The tumor DNA dynamics during NAC (tumor DNA either remained detectable or was cleared) for plasma samples remained significantly associated with NAC response (18) in this extended cohort (**Fig. 4A**). utDNA dynamics for urine supernatants was also significantly associated with NAC response, but not tdDNA from urine pellets (**Fig. 4B** and **C** and Supplementary Fig. S13). The response assessment for NAC reflects the local tumor response (pathological evaluation), so we next investigated the outcomes of the patients following RC to assess the response on distant micrometastatic disease. Here, we found that plasma ctDNA dynamics was strongly associated with RFS with particularly poor outcome for patients where ctDNA remained detectable (**Fig. 4D**). We did not observe an association between RFS and urine pellet tdDNA dynamics (**Fig. 4E**). For urine supernatants, as for plasma, we observed a strong association with RFS and a remarkable recurrence rate of 0% for patients with utDNA clearance (**Fig. 4F**). Interestingly, a combination of tumor DNA dynamics of plasma samples and urine supernatants showed concordance in 71% (17/24) of patients (**Fig. 4G**). The combination showed a potential for treatment response monitoring with concordant tumor DNA dynamics being associated with response to treatment (**Fig. 4H**) and for risk stratification of patients, as demonstrated by the difference in RFS (**Fig. 4I**).

The overall effect of NAC was reflected by a decrease in detectable mutations in residual tumors from RC compared with the primary tumor (See Materials and Methods and Supplementary Fig. S2).

Discussion

Treatment with NAC represents a clinical scenario in need of real-time monitoring to assess whether treatment is effective or initiation of alternative treatment would be optimal. Plasma samples have demonstrated promising utility based on a strong association between clearance of ctDNA and response to NAC, which importantly can be evaluated before RC is carried out (18). In addition, plasma ctDNA clearance has been associated with improved outcome following RC (18). These observations were further substantiated with the expanded patient cohort in this study. Noteworthy, tracking of ctDNA in plasma samples during treatment is only possible in the subset of patients with detectable ctDNA before initiation of NAC treatment, which in this study amounted to approximately 43%. This number could also point to the patients that actually need systemic treatment because of disseminated disease. However, it is not clear how well the ctDNA detection methods actually capture micrometastatic disease. A recent study indicated that current methods may only capture relatively large metastatic lesions (40). The similar positive detection rates reached 85% and 89% for urine pellets and supernatants, respectively. This highlights that urine samples could provide a critical component in liquid biopsy-based treatment monitoring for patients with MIBC treated with NAC simply based on the markedly higher detection rates. Importantly, we demonstrated an association between utDNA dynamics in urine supernatants and a similar trend in tdDNA from urine pellets pointing to a potential future role for urine-based treatment response monitoring. Interestingly, we observed a particularly good outcome for patients with urine supernatant utDNA clearance. This observation persisted when combining plasma and urine supernatant tumor DNA measurements and highlights a potentially predictive and prognostic value of a combinatorial liquid biopsy-based approach for monitoring of response, where a local and systemic response measure is used in combination. However, the observations require validation in larger prospective cohorts. Surprisingly, tumor DNA was identified in both urine supernatants and pellets in samples obtained at visits with no concurrent tumors. This might be due to tumor lesions being missed or from release of tumor DNA from mutant clones present in presumably normal appearing urothelium (41). However, recent studies using next-generation sequencing or digital droplet PCR have identified utDNA obtained at visits with no concurrent tumor or concurrent low-grade non-invasive tumors (23, 31, 42). In addition, utDNA was not identified in a subset of samples obtained at visits with MIBC. This has similarly been observed in a recent study by Chauhan and colleagues (19); however, the panel-based approach for tumor DNA detection in this study could imply that the lack of tumor DNA detection is for technical reasons, that is, tumor-specific variants were not queried. Furthermore, urine samples represent a sample type with inherent variability in composition and concentration, which both could have implications for the level and detectability of tumor DNA, which is also reflected in the urine test sensitivities and specificities observed in this study. Interestingly, we observed no variation in tumor DNA detection rates and tumor DNA level across a wide range of cfDNA amounts. However, we did observe a correlation between cfDNA levels and several parameters assessed using urine dipstick data. The erythrocyte level was in line with this associated with the utDNA call status of samples that aligns with hematuria as a frequent symptom of bladder cancer. Collectively, this demonstrates the extraordinary challenges created by the highly variable composition of urine samples. Future studies of urine-based liquid biopsy analysis should pursue further optimization of collection timing and procedures. A limitation to the study is the different technologies applied for plasma ctDNA analysis. Both use a patient-specific mutation selection approach based on WES data followed by targeted enrichment and sequencing, but differ in the enrichment strategies, variant calling, and read-depth. Consequently, there are differences in the LOD of the applied methods. Importantly, all samples from single patients were analyzed with the same method.

In conclusion, we assess the potential for treatment response and outcome prediction by liquid biopsies collected in the pre-surgical setting for patients with MIBC. We validated previously observed prognostic and predictive features of plasma ctDNA analysis and similarly demonstrated prognostic and predictive power for urine supernatant utDNA dynamics based on samples collected before, during and after NAC treatment. Importantly, tumor DNA dynamics analysis provides a real-time assessment that could provide clinicians with information on treatment efficacy during treatment. This may ultimately be used for guiding treatment continuation and potentially to inform about bladder sparing strategies. However, these scenarios need to be tested in new clinical trials.

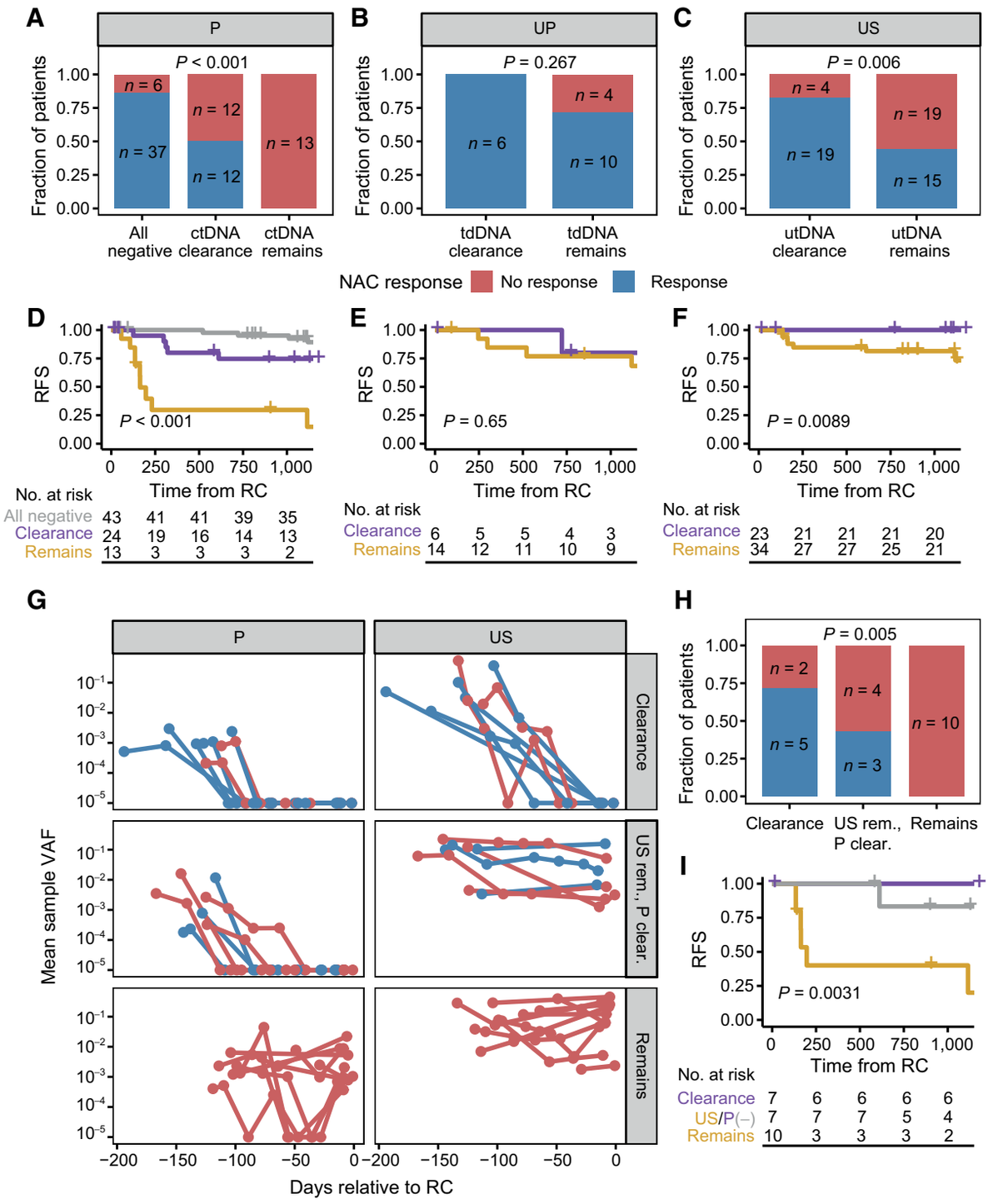

Figure 4.

Tumor DNA dynamics correlate with treatment response and outcome. **A–C,** Association between tumor DNA dynamics and neoadjuvant chemotherapy (NAC) response for (**A**) plasma, (**B**) urine pellet, and (**C**) urine supernatant. Tumor DNA clearance was defined as tumor DNA going from detectable to non-detectable and tumor DNA remains was defined as tumor DNA remaining detectable. **D–F,** Kaplan–Meier survival analysis of tumor DNA dynamics groups and recurrence-free survival (RFS) for (**D**) plasma, (**E**) urine pellet, and (**F**) urine supernatant. **G,** Detailed overview of tumor DNA dynamics during NAC for patients with information available for both plasma and urine supernatant. Overviews were split according to sample type and agreement between sample-type tumor DNA dynamics. **H,** Association between combined plasma and urine supernatant tumor DNA dynamics and NAC response. **I,** Kaplan–Meier survival analysis of combined plasma and urine supernatant tumor DNA dynamics groups and RFS.

Authors' Disclosures

J.B. Jensen reports grants from Novo Nordisk Foundation and Danish Cancer Association during the conduct of the study. L. Dyrskjøt reports grants and non-financial support from AstraZeneca and Natera and grants from Novo Nordisk Foundation and The Danish Cancer Society during the conduct of the study as well as grants and personal fees from Ferring, grants from Photocure, grants and non-financial support from C2i Genomics, and personal fees from Urogen and BioXpedia outside the submitted work. No disclosures were reported by the other authors.

Authors' Contributions

E. Christensen: Conceptualization, data curation, formal analysis, validation, investigation, visualization, methodology, writing–original draft, writing–review and editing. **I. Nordentoft:** Conceptualization, data curation, formal analysis, validation, investigation, visualization, methodology, writing–original draft, writing–review and editing. **K. Birkenkamp-Demtröder:** Conceptualization, data curation, writing–review and editing. **S.K. Elbæk:** Formal analysis, visualization, writing–review and editing. **S.V. Lindskrog:** Visualization, writing–review and editing. **A. Taber:** Data curation, writing–review and editing. **T.G. Andreasen:** Data curation, writing–review and editing. **T. Strandgaard:** Data curation, writing–review and editing. **M. Knudsen:** Data curation, software, methodology, writing–review and editing. **P. Lamy:** Data curation, software, formal analysis, methodology, writing–review and editing. **M. Agerbæk:** Data curation, writing–review and editing. **J.B. Jensen:** Resources, data curation, writing–review and editing. **L. Dyrskjøt:** Conceptualization, resources, supervision, funding acquisition, investigation, writing–original draft, project administration, writing–review and editing.

Acknowledgments

We would like to thank all technical personnel at the Departments of Molecular Medicine, Urology, and Oncology, Aarhus University Hospital, for sample handling and processing.

The publication costs of this article were defrayed in part by the payment of publication fees. Therefore, and solely to indicate this fact, this article is hereby marked "advertisement" in accordance with 18 USC section 1734.

Note

Supplementary data for this article are available at Clinical Cancer Research Online (http://clincancerres.aacrjournals.org/).

Received October 25, 2022; revised January 4, 2023; accepted February 8, 2023; published first February 13, 2023.

References

1. The International Agency for Research on Cancer (IARC). Global Cancer Observatory. [cited 2022 Apr 4]. Available from: https://gco.iarc.fr/
2. Witjes JA, Bruins HM, Cathomas R, Compérat EM, Cowan NC, Gakis G, et al. European association of urology guidelines on muscle-invasive and metastatic bladder cancer: summary of the 2020 guidelines. Eur Urol 2021;79:82–104.
3. Waingankar N, Jia R, Marqueen KE, Audenet F, Sfakianos JP, Mehrazin R, et al. The impact of pathologic response to neoadjuvant chemotherapy on conditional survival among patients with muscle-invasive bladder cancer. Urol Oncol 2019; 37:572.
4. Yin M, Joshi M, Meijer RP, Glantz M, Holder S, Harvey HA, et al. Neoadjuvant chemotherapy for muscle-invasive bladder cancer: a systematic review and two-step meta-analysis. Oncologist 2016;21:708–15.
5. Yuh BE, Ruel N, Wilson TG, Vogelzang N, Pal SK. Pooled analysis of clinical outcomes with neoadjuvant cisplatin and gemcitabine chemotherapy for muscle-invasive bladder cancer. J Urol 2013;189:1682–6.
6. Advanced Bladder Cancer (ABC) Meta-analysis Collaboration. Neoadjuvant chemotherapy in invasive bladder cancer: update of a systematic review and meta-analysis of individual patient data advanced bladder cancer (ABC) meta-analysis collaboration. Eur Urol 2005;48:202–5.
7. Teo MY, Bambury RM, Zabor EC, Jordan E, Al-Ahmadie H, Boyd ME, et al. DNA damage response and repair gene alterations are associated with improved survival in patients with platinum-treated advanced urothelial carcinoma. Clin Cancer Res 2017;23:3610–8.
8. Van Allen EM, Mouw KW, Kim P, Iyer G, Wagle N, Al-Ahmadie H, et al. Somatic ERCC2 mutations correlate with cisplatin sensitivity in muscle-invasive urothelial carcinoma. Cancer Discov 2014;4:1140–53.
9. Plimack ER, Dunbrack RL, Brennan TA, Andrake MD, Zhou Y, Serebriiskii IG, et al. Defects in DNA repair genes predict response to neoadjuvant cisplatin-based chemotherapy in muscle-invasive bladder cancer. Eur Urol 2015;68:959–67.
10. Taber A, Christensen E, Lamy P, Nordentoft I, Prip F, Lindskrog SV, et al. Molecular correlates of cisplatin-based chemotherapy response in muscle-invasive bladder cancer by integrated multi-omics analysis. Nat Commun 2020;11:4858.
11. Choi W, Porten S, Kim S, Willis D, Plimack ER, Hoffman-Censits J, et al. Identification of distinct basal and luminal subtypes of muscle-invasive bladder cancer with different sensitivities to frontline chemotherapy. Cancer Cell 2014; 25:152–65.
12. Seiler R, Ashab HAD, Erho N, van Rhijn BWG, Winters B, Douglas J, et al. Impact of molecular subtypes in muscle-invasive bladder cancer on predicting response and survival after neoadjuvant chemotherapy. Eur Urol 2017;72: 544–54.
13. Kamoun A, de Reyniès A, Allory Y, Sjödahl G, Robertson AG, Seiler R, et al. A Consensus molecular classification of muscle-invasive bladder cancer. Eur Urol 2020;77:420–33.
14. Powles T, Assaf ZJ, Davarpanah N, Banchereau R, Szabados BE, Yuen KC, et al. ctDNA guiding adjuvant immunotherapy in urothelial carcinoma. Nature 2021; 595:432–7.
15. Bettegowda C, Sausen M, Leary RJ, Kinde I, Wang Y, Agrawal N, et al. Detection of circulating tumor DNA in early- and late-stage human malignancies. Sci Transl Med 2014;6:224ra24.
16. Diehl F, Schmidt K, Choti MA, Romans K, Goodman S, Li M, et al. Circulating mutant DNA to assess tumor dynamics. Nat Med 2008;14:985–90.
17. Birkenkamp-Demtröder K, Christensen E, Nordentoft I, Knudsen M, Taber A, Høyer S, et al. Monitoring treatment response and metastatic relapse in advanced bladder cancer by liquid biopsy analysis. Eur Urol 2018;73:535–40.
18. Christensen E, Birkenkamp-Demtröder K, Sethi H, Shchegrova S, Salari R, Nordentoft I, et al. Early detection of metastatic relapse and monitoring of therapeutic efficacy by ultra-deep sequencing of plasma cell-free DNA in patients with urothelial bladder carcinoma. J Clin Oncol 2019;37:1547–57.
19. Chauhan PS, Chen K, Babbra RK, Feng W, Pejovic N, Nallicheri A, et al. Urine tumor DNA detection of minimal residual disease in muscle-invasive bladder cancer treated with curative-intent radical cystectomy: a cohort study. PLoS Med 2021;18:e1003732.
20. Patel KM, van der Vos KE, Smith CG, Mouliere F, Tsui D, Morris J, et al. Association of plasma and urinary mutant DNA with clinical outcomes in muscle-invasive bladder cancer. Sci Rep. 2017;7:5554.
21. Harris PA, Taylor R, Thielke R, Payne J, Gonzalez N, Conde JG, et al. A metadata-driven methodology and workflow process for providing translational research informatics support. J Biomed Inform 2009;42:377–81.
22. Harris PA, Taylor R, Minor BL, Elliott V, Fernandez M, O'Neal L, et al. The REDCap consortium: building an international community of software platform partners. J Biomed Inform 2019;95:103208.
23. Christensen E, Birkenkamp-Demtröder K, Nordentoft I, Høyer S, van der Keur K, van Kessel K, et al. Liquid biopsy analysis of FGFR3 and PIK3CA hotspot mutations for disease surveillance in bladder cancer. Eur Urol 2017; 71:961–9.
24. Birkenkamp-Demtröder K, Nordentoft I, Christensen E, Høyer S, Reinert T, Vang S, et al. Genomic alterations in liquid biopsies from patients with bladder cancer. Eur Urol 2016;70:75–82.
25. DePristo MA, Banks E, Poplin R, Garimella KV, Maguire JR, Hartl C, et al. A framework for variation discovery and genotyping using next-generation DNA sequencing data. Nat Genet 2011;43:491–8.
26. MuTect2 pitfalls—best practices for processing HTS data 0.0 documentation [Internet]. [cited 2022 Apr 4]. Available from: https://best-practices-for-processing-hts-data.readthedocs.io/en/latest/mutect2_pitfalls.html
27. Koboldt DC, Zhang Q, Larson DE, Shen D, McLellan MD, Lin L, et al. VarScan 2: somatic mutation and copy number alteration discovery in cancer by exome sequencing. Genome Res 2012;22:568–76.

28. Saunders CT, Wong WSW, Swamy S, Becq J, Murray LJ, Cheetham RK. Strelka: accurate somatic small-variant calling from sequenced tumor–normal sample pairs. Bioinformatics 2012;28:1811–7.
29. Wang K, Li M, Hakonarson H. ANNOVAR: functional annotation of genetic variants from high-throughput sequencing data. Nucleic Acids Res 2010;38: e164.
30. fgbio: tools for working with genomic and high-throughput sequencing data [Internet]. Github; [cited 2022 Apr 19]. Available from: http://fulcrumgenomics.github.io/fgbio/
31. Strandgaard T, Lindskrog SV, Nordentoft I, Christensen E, Birkenkamp-Demtröder K, Andreasen TG, et al. Elevated T-cell exhaustion and urinary tumor DNA levels are associated with BCG failure in patients with non–muscle-invasive bladder cancer 2022;82:646–56.
32. Robertson AG, Kim J, Al-Ahmadie H, Bellmunt J, Guo G, Cherniack AD, et al. Comprehensive molecular characterization of muscle-invasive bladder cancer. Cell 2017;171:540–56.
33. Benjamin D, Sato T, Cibulskis K, Getz G, Stewart C, Lichtenstein L. Calling Somatic SNVs and Indels with Mutect2 [Internet]. [cited 2022 Apr 19]. Available from: https://www.biorxiv.org/content/10.1101/861054v1
34. Adzhubei I, Jordan DM, Sunyaev SR. Predicting functional effect of human missense mutations using PolyPhen-2. Curr Protoc Hum Genet 2013;7: Unit7.20.
35. Reva B, Antipin Y, Sander C. Predicting the functional impact of protein mutations: application to cancer genomics. Nucleic Acids Res 2011;39:e118.
36. Bailey MH, Tokheim C, Porta-Pardo E, Sengupta S, Bertrand D, Weerasinghe A, et al. Comprehensive characterization of cancer driver genes and mutations. Cell 2018;173:371–85.
37. Rachakonda PS, Hosen I, de Verdier PJ, Fallah M, Heidenreich B, Ryk C, et al. TERT promoter mutations in bladder cancer affect patient survival and disease recurrence through modification by a common polymorphism. Proc Natl Acad Sci U S A 2013;110:17426–31.
38. Lawrence M, Gentleman R, Carey V. rtracklayer: an R package for interfacing with genome browsers. Bioinformatics 2009;25:1841–2.
39. Gerstung M, Beisel C, Rechsteiner M, Wild P, Schraml P, Moch H, et al. Reliable detection of subclonal single-nucleotide variants in tumour cell populations. Nat Commun 2012;3:811.
40. Abbosh C, Birkbak NJ, Swanton C. Early stage NSCLC—challenges to implementing ctDNA-based screening and MRD detection. Nat Rev Clin Oncol 2018;15:577–86.
41. Lawson ARJ, Abascal F, Coorens THH, Hooks Y, O'Neill L, Latimer C, et al. Extensive heterogeneity in somatic mutation and selection in the human bladder. Science 2020;370:75–82.
42. Dudley JC, Schroers-Martin J, Lazzareschi DV, Shi WY, Chen SB, Esfahani MS, et al. Detection and surveillance of bladder cancer using urine tumor DNA. Cancer Discov 2019;9:500–9.